*C*handra and *RXTE* spectroscopy of the accreting msec pulsar IGR J00291+5934

A. Paizis[1,2], M. A. Nowak[3], J. Wilms[4], T.J-L. Courvoisier[1,5], K. Ebisawa[6], J. Rodriguez[7,1] and P. Ubertini[8]

[1] *INTEGRAL* Science Data Centre, Chemin d'Ecogia 16, 1290 Versoix, Switzerland
[2] INAF-IASF, Sezione di Milano, Via Bassini 15, 20133 Milano, Italy
[3] Center for Space Research, MIT, Cambridge, MA, USA
[4] Department of Physics, University of Warwick, Coventry, CV4 7AL, UK
[5] Observatoire de Genève, 51 chemin des Mailletes, 1290 Sauverny, Switzerland
[6] NASA Goddard Space Flight Center, Code 662, Greenbelt, MD 20771, USA
[7] CEA Saclay, DSM/DAPNIA/SAp (CNRS UMR 7158 AIM) , 91191 Gif Sur Yvette, France
[8] CNR-IASF, Sezione di Roma, via del Fosso del Cavaliere 100, 00133 Roma, Italy

Abstract. We report on an observation of the recently discovered accreting millisecond X-ray pulsar IGR J00291+5934 performed with the *RXTE*-Proportional Counter Array (PCA) and *C*handra-High Energy Transmission Grating Spectrometer (HETGS). The *RXTE* data are from a two week follow-up of the source while the *C*handra observation took place around the end of the follow-up, about 12 days after the discovery of the source, when the source flux had decreased already by a factor of ten. The analysis of the *C*handra data allowed us to extract the most precise X-ray position of IGR J00291+5934, RA=00^h 29^m 03.08^s and Dec=+$59°$ $34'$ $19.2''$ ($0.6''$ error), compatible with the optical and radio ones. We find that the spectra of IGR J00291+5934 can be described by a combination of a thermal component and a power-law. Along the outburst detected by PCA, the power-law photon index shows no particular trend while the thermal component (~ 1 keV, interpreted as a hot spot on the neutron star surface) becomes weaker until non-detection. In the simultaneous observation of the weak *C*handra /*RXTE* spectrum, there is no more indication for the ~ 1 keV thermal component while we detect a colder thermal component (~ 0.4 keV) that we interpret as the emission from the cold disc. A hint for a 6.4 keV iron line is detected, together with an excess around 6.8 keV and absorption feature around 7.1 keV. The latter two features have never been detected in the spectra of accretion-driven millisecond pulsars before and, if confirmed, would suggest the presence of an expanding hot corona with high outflow velocities.

Key words. pulsars:individual IGR J00291+5934.

1. Introduction

In Low Mass X-Ray Binaries (LMXRB) hosting a neutron star, the accreting star is thought to be very old and weakly magnetised, compared to neutron star High Mass X-Ray Binaries. It is believed that in LMXRBs, the accretion disc is generally not influenced by the magnetic field and can extend very close to the neutron star surface in a slow, "spot-less" accretion. This seems to be the case for the majority of LMXRBs for which no regular pulsations have been observed (see e.g. White et al. 1995; Psaltis 2004, for a review). In a few cases though, regular X-ray pulsations have been detected with spin periods ranging from about 120 sec for GX 1+4 to less than 10 msec, e.g. for SAX J1808.4−3658. The discovery of the latter accretion-powered millisecond pulsar (APMSP) has been very important in the LMXRB evolution scenario: the existence of such systems supports the theory that LMXRBs are indeed the progenitors of millisecond radio pulsars with a low magnetic field.

Currently seven APMSPs are known. A recent review of these systems can be found in Wijnands (2005)[1]. Among them, with its 1.67 msec spin period, IGR J00291+5934 is the fastest known APMSP. Evidence for the existence of rapidly (msec) spinning neutron stars in a wider sample of LMXRBs (at least in an additional 11 systems) has been provided by the detection of nearly coherent oscillations ("burst oscillations") during type-I X-ray bursts (Chakrabarty 2004). Nevertheless, only for a few LMXRBs can we actually see the spin due to regular X-ray pulsations. The reason for this discrepancy is still debated and it is not clear why the physics at the origin of the X-ray pulsations reveals itself only through the presence of pulsations and not in the spectral and timing properties of the sources that

---

Send offprint requests to: A. Paizis: Ada.Paizis@obs.unige.ch

[1] With the exception of the very recently discovered HETE J1900.1−2455 (Morgan et al. 2005).

remain similar between APMSPs and non pulsating LMXRBs (Wijnands 2005).

In this paper we report on observations of the fastest discovered APMSP, IGR J00291+5934, performed with the *Chandra X-ray Observatory* (Weisskopf et al. 2002), 12 days after the discovery. To have a better overview of the spectral behaviour of the source prior to our observation, we have also analysed the available *Rossi X-ray Timing Explorer* (*RXTE* ; Jahoda & PCA Team 1996) observations, part of which were simultaneous to our 18 ksec *Chandra* observation.

The paper is organised as follows: in section two we give an overview of the current knowledge of IGR J00291+5934 from its discovery. In section three we present our observations and data reduction methods. In section four we present our results that are then discussed in the last section.

2. IGR J00291+5934

IGR J00291+5934 was discovered by the *INTErnational Gamma-Ray Astrophysics Laboratory* (INTEGRAL; Winkler et al. 2003) on December 2nd 2004, during routine monitoring of the Galactic plane (Eckert et al. 2004). Follow-up observations with *RXTE* revealed the presence of coherent pulsations at ~598.89 Hz (Markwardt et al. 2004) with an energy dependent fractional amplitude. Further analysis and observations with *RXTE* showed that the neutron star is in a 8844 s (2.45 h) orbit. The upper limit of 0.16 $M_\odot$ on the mass of the companion star in IGR J00291+5934 implies that the companion is most probably a hot brown dwarf (Galloway et al. 2005).

The outburst X-ray spectrum could be fitted with an absorbed power-law with Γ = 1.8 and fixed column density N_H=2×10^{21} cm^{-2} for *INTEGRAL* (Shaw et al. 2005) and Γ = 1.7 and measured column density N_H=1.7×10^{21} cm^{-2} for *RXTE* (Galloway et al. 2005). More physical models (thermal Comptonisation) led to poorly constrained electron temperatures with a cut-off between 80–120 keV (Shaw et al. 2005). Jonker et al. (2005) observed IGR J00291+5934 with *Chandra* one month after the discovery of the source, likely at its quiescent flux level, obtaining a 0.5–10 keV flux of ~10^{-13} erg cm^{-2} s^{-1} and a neutron star effective temperature of ~0.3 keV.

Inspection of the *RXTE*/ASM archive showed that the source was likely also active in the past on two occasions, leading to a tentative recurrence time of about 3 years (Remillard 2004).

Observations with ground based telescopes allowed the counterparts at optical and radio wavelengths to be discovered (Pooley 2004; Fender et al. 2004; Fox & Kulkarni 2004). The most accurate optical position of the source is RA=00^h 29^m 03.06^s and Dec=+59° 34′ 19.0″ (0.5″ uncertainty) (Fox & Kulkarni 2004).

3. Observations and data reduction

An X-ray intensity history of the 2004 outburst of IGR J00291+5934 is presented in Fig. 1, where the *INTEGRAL* detection followed by the *RXTE* follow-up are
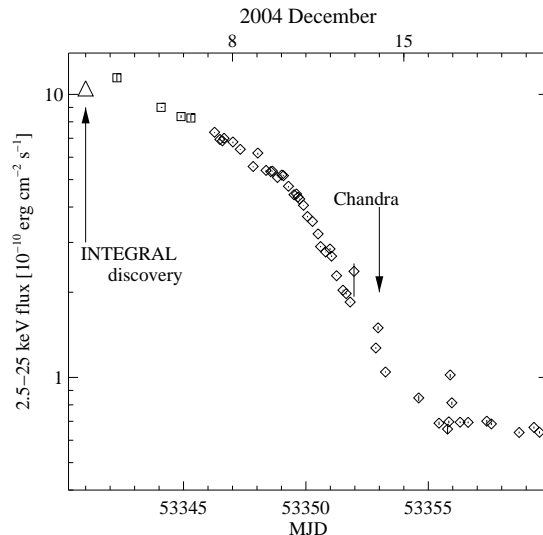

Fig. 1. X-ray intensity of IGR J00291+5934 throughout the 2004 outburst. The open triangle indicates the discovery with *INTEGRAL* . The 2.5–25 keV PCA flux evolution is shown (open squares).The time of our *Chandra* observation is indicated by the arrow in the right. After MJD 53355 the source flux is strongly influenced by residual flux and variability of (at least) the nearby V709 Cas.

shown. The time of our *Chandra* observation is indicated by the arrow on the right. As can be seen, we observed the source at a very faint flux level, after the source had decayed significantly towards quiescence.

3.1. The Chandra data

The 18 ksec *Chandra* observation of IGR J00291+5934 was performed on 2004 December 14th from 02:43:41 until 08:02:38 UT (MJD 53353). We reduced the data in a standard manner using the CIAO version 3.2 software package and CALDB version 3.0.0. The obtained spectra have been analysed with the ISIS analysis system, version 1.2.4 (Houck 2002).

We used the High Energy Transmission Grating Spectrometer, HETGS (Canizares et al. 2000). It has two sets of gratings, the High Energy Grating, HEG, and Medium Energy Grating, MEG, covering the energy ranges of 0.8–10 keV and 0.4–5.0 keV, respectively. The focal plane imager used is the Advanced CCD Imaging Spectrometer (ACIS-S), an array of six CCD detectors normally used as readout for the photons dispersed by the gratings. The CCDs were operated in a sub-array mode where only half the CCD was read out. This did not affect the dispersed spectra, but served to reduce the frame integration time from the usual 3.2 s to 1.7 s, and thus reduced the presence of pileup (see below).

Given the low signal to noise obtained, we extracted the zeroth-order (undispersed) spectrum and the first order dispersed spectra ($m = \pm 1$ for HEG and MEG) for a total of five spectra. Higher order spectra were not considered. The zeroth-order image of the source is well resolved, but is also mildly piled up (pile-up fraction of 18%). In all spectral fits wherein

we fit the zeroth-order data, we account for these effects by using the ISIS implementation of the pileup model of Davis (2001).

Within the field of view of ACIS-S we detect another source, 17′ away from the zeroth-order image of IGR J00291+5934 . The source is V709 Cas, a cataclysmic variable. The zeroth-order image of V709 Cas lies on top of the HEG $m = −1$ dispersed spectrum of IGR J00291+5934. The position of V709 Cas corresponds to the 1–1.3 keV region of the HEG $m = −1$ spectrum, that has been ignored in the spectral analysis. Outside of 1–1.3 keV, the removal of events associated with V709 Cas is extremely efficient and no contamination is occurring.

Inspection of the 5 spectra showed that the separate grating arms agree with each other. This allowed us to merge the two HEG ($m = ±1$) and MEG ($m = ±1$) spectra into two combined spectra in order to increase the signal to noise ratio. This led to three final spectra that we used in the analysis (combined first order HEG, combined first order MEG and zeroth-order). For the fit, we binned the data to obtain a minimum of 16 counts per bin for both HEG and MEG as well as a minimum number of 16 channels per bin for HEG and 8 for MEG.

The 1.67 msec pulsations cannot be detected in our data, due to the 1.7 s frame integration time in our observations. We have used both 'unbinned techniques' for searching for variability on all time scales > 1.7 s (e.g., the Bayesian Blocks method of Scargle (2005), in prep.[2]) as well as 'binned' period folding techniques to search for variability on time scales comparable to the orbital period. No statistically significant variability was found.

3.2. The RXTE data

One day after the discovery of IGR J00291+5934, a regular monitoring of the source was performed with *RXTE* via Target of Opportunity (ToO) observations starting from December 3rd until December 16th. The *RXTE* observation on December 14th was performed simultaneously to our *Chandra* pointing (from 03:08:48 to 08:53:52 UT). The *RXTE* data were extracted with the HEASOFT software, version 5.3.1 using our standard procedures (Wilms et al. 1999).

The simultaneous *Chandra*/*RXTE* fit was performed in the already mentioned ISIS package. We rebinned further the HETGS spectra to obtain a minimum number of channels per bin equal to 64 for HEG and 32 for MEG. In this way the number of PCA and HETGS data bins is comparable and during the fit similar weight is given to all the available spectra (HEG, MEG, PCA). We fitted the PCA spectra in the 3–13 keV spectral range with a 0.5% systematics and grouped the data to have a minimum signal to noise of 5. The interpretation of the PCA December 14 spectrum of IGR J00291+5934 is delicate due to the presence of (at least) the nearby cataclysmic variable V709 Cas (17′ away, see Section 3.1) that is clearly detected in the *Chandra* field of view.

To take into account the contamination from nearby sources, we subtracted the last *RXTE* pointing available from all the previous observations. The integrated 2–8 keV flux in this last PCA observation is consistent with the *Chandra* determined flux of V709 Cas alone (2.4×10^{-11} erg cm^{-2} s^{-1}), independently confirming the non-detection of IGR J00291+5934 in this observation.

4. Results

We extracted the X-ray position of IGR J00291+5934 from the zeroth-order image, obtaining RA=00^h 29^m 03.08^s and Dec=$+59°$ $34′$ $19.2″$ equinox J2000 (90% confidence error of $0.6″$[3]). This position, compatible with the optical and radio ones, was immediately announced to the community by Nowak et al. (2004).

The first order HEG and MEG spectra of IGR J00291+5934 are shown in Fig. 2. The best fit obtained, also shown in Fig. 2, is an absorbed power-law with column density[4] N_H=$(4.3\pm0.4)\times10^{21}$ cm^{-2} and $\Gamma = 2.06 \pm 0.07$ with a reduced χ^2_ν=0.79 for 431 d.o.f. The absorbed flux is 2.5×10^{-11} erg cm^{-2} s^{-1} in 0.5–8 keV and 1.9×10^{-11} erg cm^{-2} s^{-1} in 2–8 keV (∼1mCrab) with about 10% uncertainty.

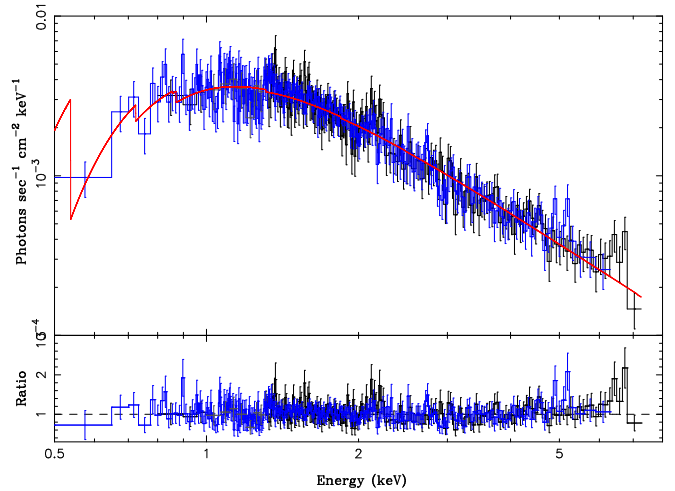**Fig. 2.** *Chandra* HEG (order m = ±1 combined, black) and MEG (order m = ±1 combined, blue) spectra of IGR J00291+5934 . The model shown is an absorbed power-law.

Residuals in the continuum are found by taking the best-fit continuum model, and then using that as a 'Bayesian prior' for the expected count rate in each bin of the *unbinned* spectrum. One can then apply the Bayesian Blocks algorithm of Scargle (2005, in prep.) to search for the most significant data residuals[5]. Using this procedure, we find the most significant

---

[2] See the implementation of this algorithm in ISIS/s-lang at http://space.mit.edu/CXC/analysis/SITAR/

[3] See http://asc.harvard.edu/cal/ASPECT/celmon/index.html

[4] The improved model for the absorption of X-rays in the interstellar medium "tbvabs" Version 1.0 was used (Wilms et al. 2000)

[5] This procedure is described in detail at: http://space.mit.edu/CXC/analysis/SITAR/bb_experiment.html

residuals to be excess emission between approximately 6.4 and 6.8 keV (1.94–1.82 Å), and an emission deficit between 7.0 and 7.2 keV (1.73–1.78 Å), as shown in Fig. 3. Fitting just the HEG spectrum between 1.5 and 3 Å, where we have grouped the data uniformly by 7 bins, and using the statistic of Cash (1979) , if we set the normalisation of the absorption line to zero and refit, the statistic increases by 10.8. This is approximately the 99.3% significance threshold. (Setting the normalisation of the emission line to zero and refitting only changes the Cash statistic value by 3.) Thus, barring systematic uncertainties of the detector, this absorption feature is approximately 3σ significant. Hints for the presence of these featues are seen in the zeroth-order spectrum as well, as we show below.
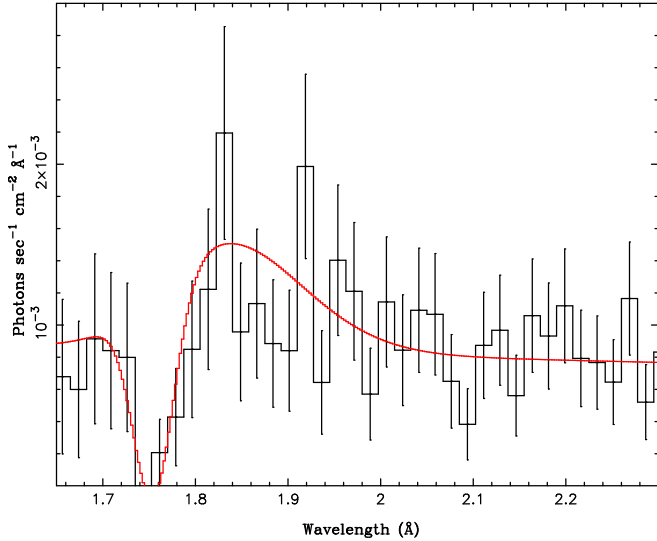

Fig. 3. HEG data uniformly rebinned by a factor of 7, where we have fitted this region with a power law plus broad line plus absorption feature. The latter is the most significant feature in our HEG spectra (approximately 99.3% significant) and is also present in the zeroth-order spectrum.

The simultaneous HETGS-PCA spectrum gave an overall harder spectrum with $\Gamma = 1.8$. The harder continuum set by PCA gave a soft excess in the *Chandra* spectrum, which was then adjusted in the fit resulting in a smaller column density ($N_H = 3.1 \times 10^{21}$ cm^{-2}). Nevertheless the fit was not very good, reduced χ^2_ν of 1.35 (163 d.o.f.), and indeed the low end of the MEG spectrum is not well described; the new N_H is lower than the value obtained fitting the *Chandra* data alone and predicts more photons in the soft end of the spectrum than what actually detected by the MEG. Furthermore, the higher end of the PCA spectrum shows a slight excess above 8 keV, meaning that the 1.8 slope is not enough for the PCA data.

To adjust for these issues, we added a soft thermal part to the spectrum (DISKBB model, Mitsuda et al. 1984) obtaining a very good description of the data (χ^2_ν=0.9, 161 d.o.f.): the PCA data are better described by the new power-law (Γ=1.7) and the softer part of the spectrum is well fitted by N_H=4.3 × 10^{21} cm^{-2} and a thermal component of $kT = 0.42$ keV (13% contribution to the absorbed 0.5–8 keV flux) that compensates for the soft

excess induced by the hard slope. Fig. 4 shows the HEG, MEG and PCA spectra of IGR J00291+5934 together with the best fit model.

The discrete feature at 2.1 keV is a known calibration origin and is due to a jump in the HETGS effective area. The excess at ~5 keV has no known instrumental origin and could be real; however, it is seen neither in the HEG nor in the zeroth-order spectrum and is less significant than the already discussed iron region features that are mirrored also in the zeroth-order spectrum.
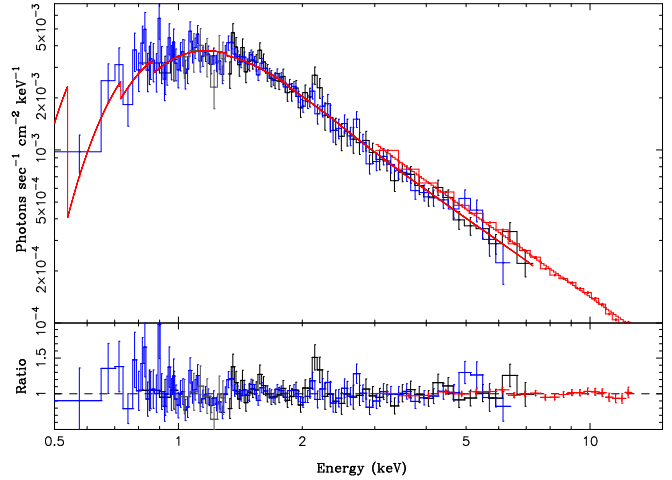

Fig. 4. HEG (black), MEG (blue) and PCA (red) spectra of IGR J00291+5934 . The fit shown is a composition of an absorbed power-law and disc blackbody.

We find that the normalisation of the PCA spectrum is about 13% higher than for *Chandra* . Between these two missions, normalisation factor up to 20% have been found before (e.g., Juett et al. 2003, and references therein). We note here that if we use a non-cleaned PCA spectrum, i.e. not corrected for the contribution of the nearby sources, we obtain a normalisation factor of 50% with respect to *Chandra*. This high value is most likely due to the contamination from nearby sources and background in the PCA spectrum.

As a last step, we included the *Chandra* zeroth-order spectrum that is affected by pile-up and thus the spectral shape from the source is distorted. Fig. 5 shows the HEG, MEG, PCA and zeroth-order count spectra. The spectral distortion due to the pile-up in the zeroth-order spectrum is visible (dip in the 1–2 keV region in the green spectrum). The emission/absorption features detected by the HEG in the iron region (already discussed, Fig. 3) are mirrored in the zeroth-order as well. The information that is lost due to pile-up can be partly recovered using kernel models that "correct" the distortions Davis (2001). Nevertheless, the result cannot be perfect and the inclusion of the zeroth-order spectrum can make the overall fit quality slightly worse. We obtain an absorbed power-law and thermal component, compatible with the previous case, with column density N_H=3.9× 10^{21} cm^{-2}, $\Gamma = 1.7$, $kT_{in} = 0.4$ keV and a reduced χ^2_ν=1.15 for 293 d.o.f. Again we find a PCA

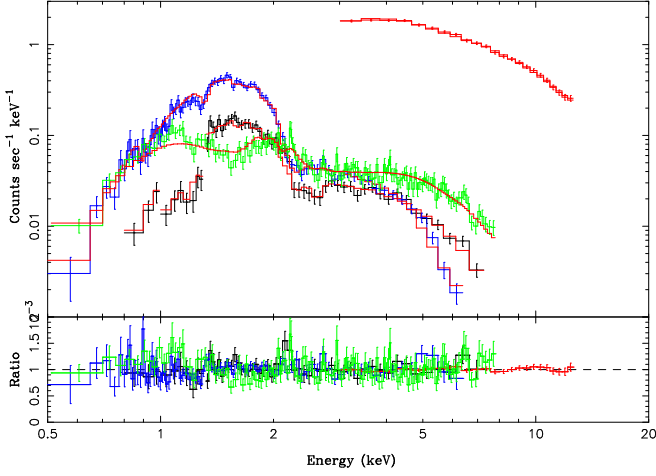normalisation of about 13% higher than for *Chandra*. Table 1 summarises the results of our spectral analysis.

Fig. 5. HEG (black), MEG (blue), PCA (red) and HETGS zeroth-order (green) count spectra of IGR J00291+5934 . Note the emission/absorption line features already discussed (Fig. 3) in both the zeroth-order and HEG spectra. The break in the HEG spectrum (data points between 1–1.3 keV) is due to the fact that in this range we have used HEG $m = +1$ alone and not the averaged $m = \pm1$ orders, due to the contamination by V709 Cas in the HEG $m = -1$ order.

5. Discussion

We have studied the spectral evolution of the accretion-powered millisecond pulsar IGR J00291+5934 with *Chandra* and *RXTE* during the December 2004 outburst that led to its discovery by *INTEGRAL*.

---

[6] This slope is adjusted to the softer 1.7 value when fitted with the *Chandra* simultaneous spectrum of December 14.

Table 1. Best fit parameters for the absorbed power-law model of the HETGS spectra of IGR J00291+5934 and for the absorbed power-law plus thermal component of the HETGS, PCA and *Chandra* zeroth-order spectra. N_H is the column density in units of 10^{21} cm^{-2}; kT_{in} is the inner temperature of the thermal (DISKBB) component; d.o.f. = degrees of freedom (the decrease in d. o. f. in the combined HEG / MEG and PCA spectrum is due to the heavy rebinning we performed in the HETGS data, see text); in all the fits we fixed to 1 HEG, MEG and zeroth-order normalisation factors. The indicated errors are at 1σ.

	HEG / MEG	HEG / MEG / PCA
N_H	4.3±0.4	$4.3^{+0.7}_{-0.5}$
Γ	2.06±0.07	1.7±0.08
kT_{in}		$0.42^{+0.07}_{-0.06}$ keV
PCA norm		1.13
reduced χ^2_ν	0.79 (431 d.o.f.)	0.9 (161 d.o.f)

	HEG / MEG PCA / 0th order
N_H	$3.9^{+0.5}_{-0.4}$
Γ	1.7±0.04
kT_{in}	0.40±0.06 keV
PCA norm	1.13
reduced χ^2_ν	1.15 (293 d.o.f.)

To have an overview of the outburst behaviour of IGR J00291+5934 before our *Chandra* observation, we analysed all the available *RXTE*/PCA observations. The PCA spectra of IGR J00291+5934 can be fitted by a combination of a thermal component (~1 keV) and power-law ($\Gamma\sim1.6$)[6]. A hint for an iron line at 6.4 keV (fixed) is detected. During the outburst, while the source is decaying, the power-law photon index shows no particular trend (unlike the normalisation that decreases significantly) while the thermal component becomes weaker and can be constrained no more by PCA. Already two days before our *Chandra* observation the *RXTE* observations are consistent with a single power-law with a marginal detection of the 6.4 keV line. We believe that in our *Chandra* spectrum we still see a residual of the disappearing 6.4 keV line as well as a soft component (0.4 keV) that cannot be constrained by PCA alone.

5.1. Long term variability

At its discovery IGR J00291+5934 had a 5–100 keV flux of about 10^{-9} erg cm^{-2} s^{-1} (Shaw et al. 2005) that decayed to about 10^{-10} erg cm^{-2} s^{-1} (extrapolated from our HETGS/PCA best fit) about 12 days later. Assuming a distance of 5 kpc (Galloway et al. 2005) we obtain that the X-ray luminosity changed from $L_X\sim10^{36}$ erg s^{-1} to $L_X\sim10^{35}$ erg s^{-1}. This corresponds to a change from ~0.01 to ~0.001 L_{Edd} that places IGR J00291+5934 at the lower end of the dim Atoll sources (~0.01–0.3 L_{Edd}), similarly to other APMSPs. Such a peak luminosity is very low if we consider the bright neutron star X-ray transients (XRTs) that display outbursts with peak luminosities of $L_X\sim10^{37}$-10^{38} erg s^{-1}. The history lightcurve of IGR J00291+5934 from the *RXTE*/ASM indicates that the flux measured at the time of the discovery is indeed the peak of the outburst but unfortunately, the distance to IGR J00291+5934 is not well constrained and we cannot be sure of the absolute value. It may seem reasonable to expect that the peak luminosity is indeed low: APMSPs are very compact systems, the disc outer radius R is relatively small compared to wider orbit LMXRBs and this limits the total disc mass ($\propto R^3$) that can build up in quiescence. When the outburst is triggered, the mass accretion onto the central object is $\propto R^2$ (Gierliński et al. 2002, and references therein). Nevertheless, things are not so straightforward and there are cases where the above scenario does not hold, e.g. in the case of the ultra compact (11.4 minute period) LMXRB 4U 1820−30 that can still reach X-ray luminosities

higher than a few times 10^{37} erg s^{-1} (Ballantyne & Strohmayer 2004).

APMSPs differ from the bright XRTs also in the quiescent luminosity: standard XRTs range between $L_X \sim 10^{32}$-10^{33} erg s^{-1} (Campana et al. 2002) while APMSPs seem to be dimmer than $\sim 10^{32}$ erg s^{-1}(Wijnands 2005). Our *Chandra* measurement of IGR J00291+5934 gives a 0.5–8 keV flux of $\sim 10^{-11}$ erg cm^{-2} s^{-1}that, compared to the 0.5–10 keV flux of $\sim 10^{-13}$ erg cm^{-2} s^{-1}by Jonker et al. (2005), clearly shows that we detected IGR J00291+5934 during its outburst decay, prior to its quiescent state.

5.2. The spectral continuum

The study of the other APMSPs has shown that during the outburst the spectra can be well fitted by a two component model, a soft thermal component and a harder one. In general the soft component is interpreted as blackbody emission from a heated hot spot on the neutron star, responsible for the X-ray pulsations, and ranges within about 0.6–1 keV (see e.g. Gierliński et al. 2002; Gierliński & Poutanen 2005; Juett et al. 2003). The harder component is interpreted as thermal Comptonization by a plasma heated by the accretion shock as the material, collimated by the magnetic field, impacts onto the neutron star surface. The source of seed photons for Comptonisation seems to be either the hot spot itself (Gierliński & Poutanen 2005) or the colder accretion disc (Titarchuk et al. 2002).

In our analysis, we find that the spectra of IGR J00291+5934 can be fitted by a combination of a thermal component and a power-law. Along the outburst, while the source is decaying, the power-law photon index shows no particular trend while the thermal component becomes weaker and can be constrained no more by PCA. At this point, we obtained our *Chandra* observation and the simultaneous weak *Chandra/RXTE* spectrum can be well described by the combination of a colder thermal component ($kT_{in} = 0.4$ keV instead of ~ 1 keV) and a power-law. The presence of the power-law means that if there is a cut-off in the spectrum, then this occurs at higher energies than the HETGS/PCA range and we are not able to constrain it. A Comptonisation model in our data gives a poorly constrained Comptonising plasma temperature of about 50 keV. The presence of the thermal component means that not all the available soft photons go through the Comptonising medium, instead there are parts that are seen directly, similarly to what was found in other APMSPs in outburst, Miller et al. (2003) and Gierliński & Poutanen (2005) on XTE J1751−305, Gierliński et al. (2002) on SAX J1808.4−3658 and Juett et al. (2003) on XTE J0929−314.

We interpret the evolution we see in PCA data and the final simultaneous PCA/*Chandra* spectral properties in the following way: at the on-set of the outburst the accreting matter is channelled onto the neutron star surface and a hot spot is created. We have indications for the hot spot in the early PCA data with a thermal component around 1 keV that is likely to be responsible for the pulsations detected by Galloway et al. (2005). The disc is colder (<1 keV) and we do not detect it directly in

the PCA spectra alone, but we see its effect in a hint for the 6.4 keV line in the PCA data, most likely originating from irradiation of the cold accretion disc by the X-ray source.[7] Along the outburst, the hot spot becomes progressively weaker and already 10 days after the on-set of the outburst we are not able to constrain it with PCA anymore. This is consistent with the fact that Galloway et al. (2005) detect no pulsations in the last phases of the outburst. The disc is likely becoming colder as it is illuminated by the fading X-ray source and is possibly receding after the outburst, similarly to other LMXRBs in which at a low accretion rate, the disc is more distant from the compact object and the overall spectrum is hard. At the time of our *Chandra* observation the hot spot (along with its pulsations) is most likely off and we detect a cold accretion disc around 0.4 keV.

5.3. Discrete features in the spectrum

Despite the regular search for discrete features in APMSPs in the past, no line was found besides the 6.4 keV one in SAX J1808.4−3658 (Gierliński et al. 2002). In our study, a hint for an iron Kα line (fixed at 6.4 keV) is detected in the PCA observations, while a marginally significant excess in the 6.4–6.8 keV region and a 3σ significance deficit around 7.1 keV are detected in both the HEG and zeroth-order *Chandra* spectra (Figs. 3 and 5). Emission lines at 6.4 keV have been observed from many X-ray pulsars and are believed to be produced by fluorescence of weakly ionised iron (less than Fe XV). A likely candidate for this cold matter is the accretion disc that can be also responsible for the iron K-edge ~ 7.1 keV feature we detect in the spectrum. The emission line that we detect around 6.8 keV (if real) would require the presence of a highly ionised, i.e. hot, corona in IGR J00291+5934, consistent with the high plasma temperature (>10 keV) inferred from the spectral study performed here, as well as in Shaw et al. (2005). This scenario would require a different medium for each feature of Fig. 3 (cold disc for the 7.1 keV feature and hot corona for the 6.8 keV one).

Another possible, although speculative, interpretation of the discrete features in Fig. 3 could be the following: the emission feature we detect around 6.8 keV could be the redshifted part of the 6.97 keV line (expected from Fe XXVI) while the absorption feature around 7.1 keV could be the blueshifted 6.97 keV line. In this scenario we would basically obtain that the 6.4 keV line is produced by the cold disc while the 6.8 and 7.1 keV lines are a P-Cygni profile from an expanding hot corona with outflow velocities of about 6000 km/sec. Such (and higher) outflow velocities are possible and have already been observed in cataclysmic variables (e.g., Woods et al. 1992) and in the X-ray binary SS433 (Migliari et al. 2005). The P-Cygni profile scenario is consistent with all the available data we currently have on IGR J00291+5934. However, the relatively low

---

[7] A direct simultaneous measure of the hot spot and disc has been reported in the case of the APMSP XTE J1751−305 by Gierliński & Poutanen (2005) where two soft components were detected in the broad-band *XMM-Newton/RXTE* spectrum: ~ 0.6 keV, associated to the disc and ~ 1 keV, the hot spot.

statistical significance of the discrete features does not allow us to firmly establish this interpretation and underlines the importance of obtaining quick follow-ups of these transient events.

References

Ballantyne, D. R. & Strohmayer, T. E. 2004, ApJ, 602, L105

Campana, S., Stella, L., Gastaldello, F., et al. 2002, ApJ, 575, L15

Canizares, C. R., Huenemoerder, D. P., Davis, D. S., et al. 2000, ApJ, 539, L41

Cash, W. 1979, ApJ, 228, 939

Chakrabarty, D. 2004, Binary Radio Pulsar ASP Conference Series, astroph-0408004

Davis, J. E. 2001, ApJ, 562, 575

Eckert, D., Walter, R., Kretschmar, P., et al. 2004, The Astronomer's Telegram, 352, 1

Fender, R., De Bruyn, G., Pooley, G., & Stappers, B. 2004, The Astronomer's Telegram, 361, 1

Fox, D. B. & Kulkarni, S. R. 2004, The Astronomer's Telegram, 354, 1

Galloway, D. K., Markwardt, C. B., Morgan, E. H., Chakrabarty, D., & Strohmayer, T. E. 2005, ApJ, 622, L45

Gierliński, M., Done, C., & Barret, D. 2002, MNRAS, 331, 141

Gierliński, M. & Poutanen, J. 2005, (astro-ph/0411716)

Houck, J. C. 2002, in High Resolution X-ray Spectroscopy with XMM-Newton and Chandra

Jahoda, K. & PCA Team. 1996, Bulletin of the American Astronomical Society, 28, 1285

Jonker, P. G., Campana, S., Steeghs, D., et al. 2005, astro-ph/0505120

Juett, A. M., Galloway, D. K., & Chakrabarty, D. 2003, ApJ, 587, 754

Markwardt, C. B., Swank, J. H., & Strohmayer, T. E. 2004, The Astronomer's Telegram, 353, 1

Migliari, S., Fender, R. P., Blundell, K. M., Méndez, M., & van der Klis, M. 2005, MNRAS, 358, 860

Miller, J. M., Wijnands, R., Méndez, M., et al. 2003, ApJ, 583, L99

Mitsuda, K., Inoue, H., Koyama, K., et al. 1984, PASJ, 36, 741

Morgan, E., Kaaret, P., & Vanderspek, R. 2005, The Astronomer's Telegram, 523, 1

Nowak, M. A., Paizis, A., Wilms, J., et al. 2004, The Astronomer's Telegram, 369, 1

Pooley, G. 2004, The Astronomer's Telegram, 355, 1

Psaltis, D. 2004, astro-ph/0410536, to appear in "Compact Stellar X-ray Sources", eds. W.H.G. Lewin and M. van der Klis

Remillard, R. 2004, The Astronomer's Telegram, 357, 1

Scargle, J. D. 2005, in preparation

Shaw, S. E., Mowlavi, N., Rodriguez, J., et al. 2005, A&A, 432, L13

Titarchuk, L., Cui, W., & Wood, K. 2002, ApJ, 576, L49

Weisskopf, M. C., Brinkman, B., Canizares, C., et al. 2002, PASP, 114, 1

White, N. E., Nagase, F., & Parmar, A. N. 1995, From *X-Ray Binaries*, ed. W. E. G. Lewin, J. van Paradijs and van den Heuvel E. P. J., Cambridge

Wijnands, R. 2005, Nova Science Publishers (NY) volume "Pulsars New Research", astroph-0501264

Wilms, J., Allen, A., & McCray, R. 2000, ApJ, 542, 914

Wilms, J., Nowak, M. A., Dove, J. B., Fender, R. P., & di Matteo, T. 1999, ApJ, 522, 460

Winkler, C., Courvoisier, T. J.-L., Di Cocco, G., et al. 2003, A&A, 411, L1

Woods, J. A., Verbunt, F., Collier Cameron, A., Drew, J. E., & Piters, A. 1992, MNRAS, 255, 237